ARTICLE

Three-Dimensional Self-Assembly of Graphene Oxide and DNA into Multifunctional Hydrogels

Yuxi Xu, Qiong Wu, Yiqing Sun, Hua Bai, and Gaoquan Shi*

Department of Chemistry, Tsinghua University, Beijing 100084, People's Republic of China

ABSTRACT Graphene and its functionalized derivatives are unique and versatile building blocks for self-assembly to fabricate graphene-based functional materials with hierarchical microstructures. Here we report a strategy for three-dimensional self-assembly of graphene oxide sheets and DNA to form multifunctional hydrogels. The hydrogels possess high mechanical strength, environmental stability, and dye-loading capacity, and a exhibit self-healing property. This study provides a new insight for the assembly of functionalized graphene with other building blocks, especially biomolecules, which will help rational design and preparation of hierarchical graphene-based materials.

KEYWORDS: graphene oxide · DNA · three-dimensional self-assembly · multifunctional · hydrogel

Graphene and its functionalized derivatives are versatile building blocks for carbon-based materials, owing to their unique two-dimensional (2D) structure and excellent physical and chemical properties.[1−3] Recent work has demonstrated that self-assembly is a powerful technique for constructing hierarchical graphene-based architectures with novel functions.[4−8] Particularly, self-assembly of nanoscale graphene into macroscopic materials can translate the properties of individual graphene sheets into the resulting macrostructures which showed numerous breakthrough applications in optoelectronics,[9] energy-storage,[10−12] and biomedicine.[13−15] For example, transparent conducting membranes[16−19] and strong layered paperlike materials[20−23] have been prepared by various 2D self-assembly methods including flow-directed self-assembly, layer-by-layer deposition, and Langmuir−Blodgett technique. Recently, we have realized three-dimensional (3D) self-assembly of 2D reduced graphene oxide (reduced GO) sheets into hydrogels with excellent mechanical, thermal, and electrochemical properties *via* a one-step hydrothermal strategy.[24] A noble-metal-promoted 3D macro-assembly of single-layered GO sheets has also been demonstrated by Wang *et al.* through a similar process.[25] However, the work on 3D self-assembly of graphene and its functionalized derivatives is still limited;[24−28] more facile and mild assembling strategies are needed for fabricating multifunctional 3D graphene macrostructures. As an important class of biological building blocks, DNA bas been applied for noncovalent functionalization or assembly of GO sheets in a 2D assembly manner. In these GO/DNA composite assemblies, single-stranded DNA (ssDNA) chains flatly lay on the surfaces of GO sheets *via* $\pi-\pi$ stacking interactions.[14,29−32] Nevertheless, the 3D assembly behavior of GO and DNA has not yet been clearly revealed. In this paper, we describe a convenient route for 3D self-assembly of GO sheets and *in situ* formed ssDNA chains into multifunctional hydrogels. The GO/DNA composite self-assembled hydrogel (GO/DNA SH) with high-water-content (~99%) is not only mechanically strong but is also self-healing and has high environmental stability and dye-loading capacity.

RESULTS AND DISCUSSION

The typical GO/DNA SH can be readily prepared by mixing equal volumes of the aqueous dispersion of GO (6 mg mL^{-1}) (Supporting Information, Figure S1) and the aqueous solution of double-stranded DNA (dsDNA) (10 mg mL^{-1}) followed by heating the homogeneous mixture at 90 °C for 5 min (Figure 1). During the heating process, the dsDNA was unwound to ssDNA (Figure 2a) and the *in situ* formed ssDNA chains bridged adjacent GO sheets *via* strong noncovalent interactions. As a re-

*Address correspondence to gshi@tsinghua.edu.cn.

Received for review October 10, 2010 and accepted November 11, 2010.

Published online November 16, 2010. 10.1021/nn1027104

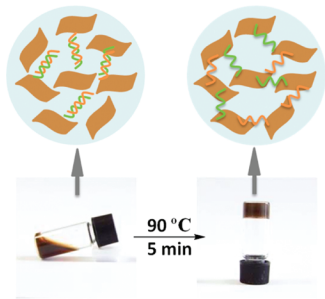

Figure 1. The procedure of preparing GO/DNA SH and the proposed gelation mechanism.

sult, a stable SH built of GO sheets and ssDNA chains was formed (Figure 1). The binding of ssDNA to GO sheets was confirmed by Raman spectroscopy. The tangential G Raman band of the GO sheets in GO/DNA SH (1589 cm^{-1}) was found to be red-shifted for about 6 cm^{-1} compared with those of pure GO and a GO/dsDNA mixture (1595 cm^{-1}, Figure 2b). This phenomenon can be attributed to the charge transfer from the nucleic acid bases of DNA chains to GO sheets,[33] similar to the case of wrapping carbon nanotubes by DNA.[34] It was also found that the modulus of the aqueous mixture of GO and dsDNA increased dramatically as its temperature was increased from 40 to 90 °C, which is within the temperature scale of dsDNA unwinding (Figure 2a). This fact indicates that the unwinding of dsDNA is the key factor for the formation of SH and strongly supports the mechanism proposed in Figure 1. The observed difference between the two curves in Figure 2a probably because of the small molecular weight dsDNA chains with low melting temperature cannot bridge GO sheets, thus, do not have contribution to the strength of SH. On the other hand, direct addition of GO dispersion into preprepared ssDNA hot solution only produced heterogeneous hydrogels, mainly due to the fast binding of ssDNA chains to GO sheets resulted in regional gelation into particles. It is worthy of note that our strategy is also applicable for the gelation of reduced GO with restored π-network, which further confirms the proposed mechanism (Supporting Information, Figure S2).

The interior microstructures of as-prepared GO/DNA SH were imaged by scanning electron microscope (SEM) of its lyophiled samples. As shown in Figure 3a and 3b, the SH has a well-defined and interconnected 3D porous network. The pore diameters range from submicrometer to several micrometers and the pore walls consist of very thin layers of stacked GO sheets. Partial coalescing of flexible GO sheets though ssDNA binding resulted in the formation of physical cross-linking sites of the SH network. The ssDNA bridging as the driving force for 3D self-assembly of GO and DNA was further confirmed by the X-ray diffraction (XRD) patterns shown in Figure 3c. The strong characteristic 2θ peak for lyophiled GO appears at 10.6°, corresponding to a layer-to-layer stacking distance of 8.34 Å, which is consistent with our previous report.[22] In contrast,

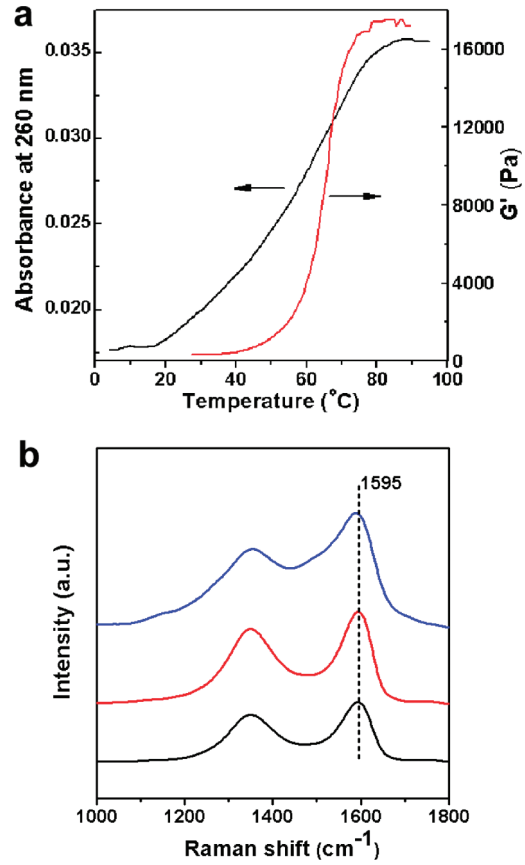

Figure 2. (a) Thermal melting curve of dsDNA monitored by absorption spectrum and temperature-dependent curve of storage modulus (G′) of SH recorded during rheological test; (b) 514 nm excited Raman spectra of GO (black), GO/dsDNA mixture before heating (red), and GO/DNA SH (blue).

there is no XRD diffraction peak for lyophiled GO/DNA SH, suggesting the absence of direct interaction or ordered stacking between GO sheets in the SH and confirming that ssDNA acted as a "glue" for binding GO sheets together to form 3D networks. This case is different from that of the self-assembled reduced GO hydrogel reported previously by us[24] (the hydrogel described in the literature was formed by π-stacking interaction between reduced GO sheets), demonstrating the diversity of 3D assembly of functionalized graphene.

Small deformation oscillatory measurements revealed that the storage modulus (G′) of the SH has a substantial elastic response with slight dependence on testing angular frequency. Furthermore, G′ is always higher than loss modulus (G′′) over the entire tested range (1−100 rad s^{-1}, Figure 3d). This result indicates that the SH has a permanent network with high degree of cross-linking. The G′ value of the typical SH was measured to be about 4.6 kPa, allowing the formation of a free-standing SH (Figure 3d inset). Although the SH contains about 99% water, its mechanical property is still impressive,[35] probably due to the cooperative contributions of inherently superior strength of GO and strong binding between ssDNA chains and GO sheets. The gelation behavior and the mechanical strength of result-

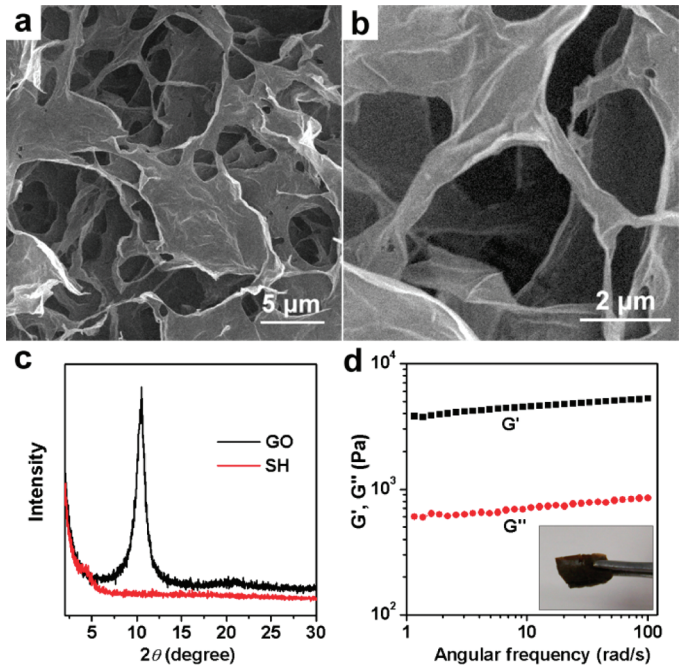

Figure 3. SEM images with low (a) and high (b) magnifications of GO/DNA SH interior microstructures; (c) XRD patterns of freeze-dried GO and GO/DNA SH; (d) dynamic rheological behavior of the typical SH prepared from the mixture of equal volume solutions of 6 mg mL^{-1} GO and 10 mg mL^{-1} dsDNA. The inset shows a free-standing GO/DNA SH.

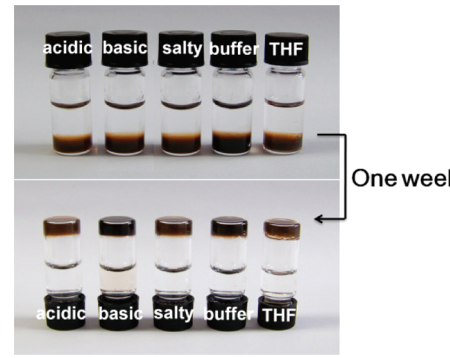

Figure 4. Effects of pH, NaCl, buffer, and organic solvent on GO/DNA SH stability. From left to right: water (pH = 2), water (pH = 13), NaCl aqueous solution (1 M), phosphate buffer (pH = 8, 10 mM) and THF. Each of the above solution (0.8 mL) was added slowly onto typical SH (0.2 mL), and the sample was allowed to stand at room temperature for one week.

ing SH depend on the concentrations of GO and dsDNA in their mixtures. It was found that raising the concentration of each component favored gelation and also improved the mechanical strength of the resulting SH (Supporting Information, Figure S3). This is mainly due to that the robustness of the 3D network was enhanced by increasing the cross-linking sites between GO sheets and DNA chains.

Unlike many other self-assembly hydrogels, our GO/DNA SH is stable in a variety of harsh conditions. As shown in Figure 4, the SH maintained its form and integrity after a 1 week immersion in strong acidic (pH 2), basic (pH 13), or salty (1 M NaCl) aqueous solution, or even in organic solvents such as tetrahydrofuran (THF). The impressive environmental stability of the SH could be attributed to the strong binding of DNA chains to GO sheets *via* multiple noncovalent interactions, including the $\pi-\pi$ stacking and hydrophobic interactions between the bases of DNA and graphitic domains of GO, as well as the electrostatic/hydrogen bonding interactions between the prime amines of bases and the oxygen-containing groups of GO.[14]

The as-prepared GO/DNA SH was tested be effective for dye adsorption. We chose safranine O as a model dye and put 0.6 mL of its aqueous solution (0.1 mg mL^{-1}) to 0.2 mL SH at room temperature. After 12 h, more than 80% of the dye was adsorbed by the SH and this value increased to nearly 100% after 24 h, as confirmed by the digital images and absorption spectra shown in Figure 5a,b. The total dye-loading capacity of the SH for safranine O was estimated to be 960 mg g^{-1} GO (Supporting Information, Figure S4), which is comparable to those of many carbon nanomaterials.[36] The high dye-loading ability of the SH is partially resulted from the strong electrostatic interactions between positively charged safranie O and negatively charged GO as well as DNA. Meanwhile, the porous structure of the SH provides a large specific surface area and abundant conjugated domains of GO to increase

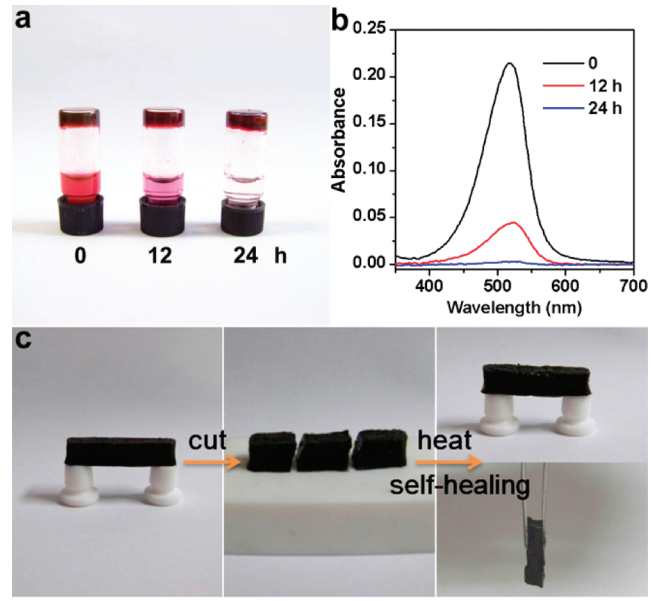

Figure 5. Photographs (a) and absorption spectra (b) of an aqueous solution of safranine O after adsorption by GO/DNA SH for different times; 0.6 mL of dye solution (0.1 mg mL^{-1}) was added onto 0.2 mL SH, and the sample was tested at room temperature. (c) Self-healing process: the as-prepared free-standing SH was cut with a razor into three small blocks and the blocks could adhere to each other by pushing the freshly formed surfaces to contact together followed by heating at 90 °C in air for 3 min.

the contact opportunity and affinity of dye molecules on GO sheets.

It is interesting to find the GO/DNA SH possesses a self-healing property. As shown in Figure 5c, a 2.5-cm-long free-standing SH was cut with a razor into three small blocks to expose fresh surfaces. Then, the blocks were pushed together to make these surfaces contact with each other, and then the whole sample was heated at 90 °C in air for 3 min. After heating treatment, the blocks adhered to each other and the resulting self-healed SH was strong enough to bridge two posts horizontally or allow vertical handle. We proposed a feasible mechanism for the self-healing phenomenon as follows. Since the excessive ssDNA in SH which is unbound or weakly bound to GO could reversibly be converted to dsDNA during the cooling process, the as-prepared SH would contain some free dsDNA in its water phase. This assumption has been confirmed by circular dichroism spectral examination of its extract (Supporting Information, Figure S5). As the fresh SH surfaces were pushed together and heated, the free dsDNA would re-unwind to yield *in situ* ssDNA which linked the adjacent GO sheets at the interfaces to repair the damage. This proposed mechanism was further confirmed by the observation that the cutting blocks could not adhere to each other without heating treatment.

CONCLUSIONS

We have developed a novel and facile 3D self-assembly method to prepare GO/DNA composite hydrogels with high mechanical strength, excellent environmental stability, high dye-adsorption capacity, and self-healing function. The multifunctionality of the SH can be attributed to the unique structures, properties, and self-assembly behavior of GO and DNA building blocks. Considering the multifunction of the hydrogels, and the biocompatibility of GO and DNA, our SH is attractive for a variety of biological and environmental applications such as tissue engineering, drug delivery, and removing organic pollutant. Furthermore, this work provides a new insight for the assembly of functionalized graphene with other building blocks, especially biomolecules, which will help rational design and fabrication of hierarchical graphene-based materials.

MATERIALS AND METHODS

Materials. Natural graphite powder (325 mesh) was purchased from Qingdao Huatai Lubricant Sealing S&T Co. Ltd. (Qingdao, China). DNA sodium salt, fish sperm (high purity grade, CAS number, 100403-24-5) was bought from Amresco Co. (Solon, USA), and its molecular weight was determined to be about 20−30 base pairs for average with a wide distribution with 20 bp DNA ladder marker (TaKaRa Co., Dalian, China). Safranine O was purchased from Alfa Aesar. All other agents were of analytical grade and obtained from Beijing Chemical Reagent Co. Water used in all experiments was purified through deionization and filtration with a Millipore purification apparatus to the resistivity higher than 18.0 MΩ cm.

Graphene Oxide (GO) Synthesis and Purification. GO was prepared by oxidation of natural graphite powder according to the modified Hummers' method.[5,37] The details are described as follows. Graphite (3.0 g) was added to concentrated sulfuric acid (70 mL) under stirring at room temperature, then sodium nitrate (1.5 g) was added, and the mixture was cooled to 0 °C. Under vigorous agitation, potassium permanganate (9.0 g) was added slowly to keep the temperature of the suspension to be lower than 20 °C. Successively, the reaction system was transferred to a 35−40 °C water bath for about 0.5 h, forming a thick paste. Then, 140 mL water was added, and the solution was stirred for another 15 min. An additional 500 mL of water was added and followed by a slow addition of 20 mL of H_2O_2 (30%), turning the color of the solution from brown to yellow. The mixture was filtered and washed with 1:10 HCl aqueous solution (250 mL) to remove metal ions, followed by repeated washing with water and centrifugation to remove the acid. The resulting solid was dispersed in water by ultrasonication for 1 h to make a GO aqueous dispersion (1 wt %). The obtained brown dispersion was then subjected to 30 min of centrifugation at 4000 rpm to remove any aggregates. Finally, it was purified by dialysis for 1 week to remove the remaining salt impurities for the following experiments.

Preparation of GO/DNA Self-Assembled Hydrogels (GO/DNA SH). Equal volumes aqueous solutions of GO and DNA with different concentrations were mixed to form homogeneous solutions and the mixtures were heated at 90 °C in oven for 5 min to yield hydrogels.

Characterization. Atomic force microscopic images were taken using a Nanoscope III MultiMode SPM (Digital Instruments) with an AS-12 ("E") scanner operated in tapping mode in conjunction with a V-shaped tapping tip (Applied Nanostructures SPM model: ACTA). The images were recorded at a scan rate of 2 Hz. The freeze-dried SH were broken to small pieces with a tweezer to expose their interior surfaces. The interior morphologies of SGHs were analyzed by a Sirion 200s scanning electron microscope (JEOL, Japan). The X-ray diffration patterns of freeze-dried SH and GO were performed by using a D8 Advance X-ray diffractometer with Cu Kα radiation (λ = 1.5418 Å, Bruker, Germany). The rheological behaviors of SH were investigated by a MCR 300 (Paar Physica) Rheometer using a 25-mm parallel-plate geometry at 25 °C. The gap distance between two plates was fixed to be 1 mm. Dynamic frequency sweep experiments were measured from 1 to 100 rad/s at a fixed oscillatory strain of 0.5%.

Acknowledgment. This work was supported by Natural Science Foundation of China (50873052, 20774056).

Supporting Information Available: Additional figures and discussion. This material is available free of charge *via* the Internet at http://pubs.acs.org.

REFERENCES AND NOTES

1. Geim, A. K. Graphene: Status and Prospects. *Science* **2009**, *324*, 1530–1534.
2. Rao, C. N. R.; Sood, A. K.; Subrahmanyam, K. S.; Govindaraj, A. The New Two-Dimensional Nanomaterial. *Angew. Chem., Int. Ed.* **2009**, *48*, 7752–7777.
3. Compton, O. C.; Nguyen, S. T. Graphene Oxide, Highly Reduced Graphene Oxide, and Graphene: Versatile Building Blocks for Carbon-Based Materials. *Small* **2010**, *6*, 711–723.
4. Li, D.; Kaner, R. B. Graphene-Based Materials. *Science* **2008**, *320*, 1170–1171.
5. Xu, Y. X.; Zhao, L.; Bai, H.; Hong, W. J.; Li, C.; Shi, G. Q. Chemically Converted Graphene Induced Molecular Flattening of 5,10,15,20-Tetrakis(1-methyl-4-pyridinio)porphyrin and Its Application for Optical

Detection of Cadmium(II) Ions. *J. Am. Chem. Soc.* **2009**, *131*, 13490–13497.
6. Guo, C. X.; Yang, H. B.; Sheng, Z. M.; Lu, Z. S.; Song, Q. L.; Li, C. M. Layered Graphene/Quantum Dots for Photovoltaic Devices. *Angew. Chem., Int. Ed.* **2010**, *49*, 3014–3017.
7. Yang, S.; Feng, X.; Wang, L.; Tang, K.; Maier, J.; Mullen, K. Graphene-Based Nanosheets with a Sandwich Structure. *Angew. Chem., Int. Ed.* **2010**, *49*, 4795–4799.
8. Bai, H.; Li, C.; Wang, X. L.; Shi, G. Q. A pH-Sensitive Graphene Oxide Composite Hydrogel. *Chem. Commun.* **2010**, *46*, 2378–2380.
9. Eda, G.; Chhowalla, M. Chemically Derived Graphene Oxide: Towards Large-Area Thin-Film Electronics and Optoelectronics. *Adv. Mater.* **2010**, *22*, 2392–2415.
10. Wang, D. W.; Li, F.; Zhao, J. P.; Ren, W. C.; Chen, Z. G.; Tan, J.; Wu, Z. S.; Gentle, I.; Lu, G. Q.; Cheng, H. M. Fabrication of Graphene/Polyaniline Composite Paper *via in Situ* Anodic Electropolymerization for High-Performance Flexible Electrode. *ACS Nano* **2009**, *3*, 1745–1752.
11. Wang, D. H.; Kou, R.; Choi, D.; Yang, Z. G.; Nie, Z. M.; Li, J.; Saraf, L. V.; Hu, D. H.; Zhang, J. G.; Graff, G. L.; Liu, J.; Pope, M. A.; Aksay, I. A. Ternary Self-Assembly of Ordered Metal Oxide-Graphene Nanocomposites for Electrochemical Energy Storage. *ACS Nano* **2010**, *4*, 1587–1595.
12. Lee, J. K.; Smith, K. B.; Hayner, C. M.; Kung, H. H. Silicon Nanoparticles-Graphene Paper Composites for Li Ion Battery Anodes. *Chem. Commun.* **2010**, *46*, 2025–2027.
13. Chen, H.; Muller, M. B.; Gilmore, K. J.; Wallace, G. G.; Li, D. Mechanically Strong, Electrically Conductive, and Biocompatible Graphene Paper. *Adv. Mater.* **2008**, *20*, 3557–3561.
14. Patil, A. J.; Vickery, J. L.; Scott, T. B.; Mann, S. Aqueous Stabilization and Self-Assembly of Graphene Sheets into Layered Bio-nanocomposites using DNA. *Adv. Mater.* **2009**, *21*, 3159–3164.
15. Park, S.; Mohanty, N.; Suk, J. W.; Nagaraja, A.; An, J. H.; Piner, R. D.; Cai, W. W.; Dreyer, D. R.; Berry, V.; Ruoff, R. S. Biocompatible, Robust Free-Standing Paper Composed of a TWEEN/Graphene Composite. *Adv. Mater.* **2010**, *22*, 1736–1740.
16. Eda, G.; Fanchini, G.; Chhowalla, M. Large-Area Ultrathin Films of Reduced Graphene Oxide as a Transparent and Flexible Electronic Material. *Nat. Nanotechnol.* **2008**, *3*, 270–274.
17. Li, X. L.; Zhang, G. Y.; Bai, X. D.; Sun, X. M.; Wang, X. R.; Wang, E.; Dai, H. J. Highly Conducting Graphene Sheets and Langmuir–Blodgett Films. *Nat. Nanotechnol.* **2008**, *3*, 538–542.
18. Cote, L. J.; Kim, F.; Huang, J. X. Langmuir–Blodgett Assembly of Graphite Oxide Single Layers. *J. Am. Chem. Soc.* **2009**, *131*, 1043–1049.
19. Biswas, S.; Drzal, L. T. A Novel Approach to Create a Highly Ordered Monolayer Film of Graphene Nanosheets at the Liquid–Liquid Interface. *Nano Lett.* **2009**, *9*, 167–172.
20. Dikin, D. A.; Stankovich, S.; Zimney, E. J.; Piner, R. D.; Dommett, G. H. B.; Evmenenko, G.; Nguyen, S. T.; Ruoff, R. S. Preparation and Characterization of Graphene Oxide Paper. *Nature* **2007**, *448*, 457–460.
21. Li, D.; Muller, M. B.; Gilje, S.; Kaner, R. B.; Wallace, G. G. Processable Aqueous Dispersions of Graphene Nanosheets. *Nat. Nanotechnol.* **2008**, *3*, 101–105.
22. Xu, Y. X.; Bai, H.; Lu, G. W.; Li, C.; Shi, G. Q. Flexible Graphene Films *via* the Filtration of Water-Soluble Noncovalent Functionalized Graphene Sheets. *J. Am. Chem. Soc.* **2008**, *130*, 5856–5857.
23. Chen, C. M.; Yang, Q. H.; Yang, Y. G.; Lv, W.; Wen, Y. F.; Hou, P. X.; Wang, M. Z.; Cheng, H. M. Self-Assembled Free-Standing Graphite Oxide Membrane. *Adv. Mater.* **2009**, *21*, 3007–3011.
24. Xu, Y. X.; Sheng, K. X.; Li, C.; Shi, G. Q. Self-Assembled Graphene Hydrogel *via* a One-Step Hydrothermal Process. *ACS Nano* **2010**, *4*, 4324–4330.
25. Tang, Z. H.; Shen, S. L.; Zhuang, J.; Wang, X. Noble-Metal-Promoted Three-Dimensional Macroassembly of Single-Layered Graphene Oxide. *Angew. Chem., Int. Ed.* **2010**, *49*, 4603–4607.
26. Liu, F.; Seo, T. S. A Controllable Self-Assembly Method for Large-Scale Synthesis of Graphene Sponges and Free-Standing Graphene Films. *Adv. Funct. Mater.* **2010**, *20*, 1930–1936.
27. Vickery, J. L.; Patil, A. J.; Mann, S. Fabrication of Graphene–Polymer Nanocomposites With Higher-Order Three-Dimensional Architectures. *Adv. Mater.* **2009**, *21*, 2180–2184.
28. Worsley, M. A.; Pauzauskie, P. J.; Olson, T. Y.; Biener, J.; Satcher, J. H.; Baumann, T. F. Synthesis of Graphene Aerogel with High Electrical Conductivity. *J. Am. Chem. Soc.* **2010**, *132*, 14067–14069.
29. Mohanty, N.; Berry, V. Graphene-Based Single-Bacterium Resolution Biodevice and DNA Transistor: Interfacing Graphene Derivatives with Nanoscale and Microscale Biocomponents. *Nano Lett.* **2008**, *8*, 4469–4476.
30. Lu, C. H.; Yang, H. H.; Zhu, C. L.; Chen, X.; Chen, G. N. A Graphene Platform for Sensing Biomolecules. *Angew. Chem., Int. Ed.* **2009**, *48*, 4785–4787.
31. Tang, Z. W.; Wu, H.; Cort, J. R.; Buchko, G. W.; Zhang, Y. Y.; Shao, Y. Y.; Aksay, I. A.; Liu, J.; Lin, Y. H. Constraint of DNA on Functionalized Graphene Improves Its Biostability and Specificity. *Small* **2010**, *6*, 1205–1209.
32. He, S. J.; Song, B.; Li, D.; Zhu, C. F.; Qi, W. P.; Wen, Y. Q.; Wang, L. H.; Song, S. P.; Fang, H. P.; Fan, C. H. Graphene Nanoprobe for Rapid, Sensitive, and Multicolor Fluorescent DNA Analysis. *Adv. Funct. Mater.* **2010**, *20*, 453–459.
33. Das, B.; Voggu, R.; Rout, C. S.; Rao, C. N. R. Changes in the Electronic Structure and Properties of Graphene Induced by Molecular Charge-Transfer. *Chem. Commun.* **2008**, *41*, 5155–5157.
34. Erdem, A.; Papakonstantinou, P.; Murphy, H. Direct DNA Hybridization at Disposable Graphite Electrodes Modified with Carbon Nanotubes. *Anal. Chem.* **2006**, *78*, 6656–6659.
35. Banerjee, S.; Das, R. K.; Maitra, U. Supramolecular Gels 'In Action'. *J. Mater. Chem.* **2009**, *19*, 6649–6687.
36. Zhuang, X.; Wan, Y.; Feng, C. M.; Shen, Y.; Zhao, D. Y. Highly Efficient Adsorption of Bulky Dye Molecules in Wastewater on Ordered Mesoporous Carbons. *Chem. Mater.* **2009**, *21*, 706–716.
37. Hummers, W. S.; Offeman, R. E. Preparation of Graphitic Oxide. *J. Am. Chem. Soc.* **1958**, *80*, 1339.